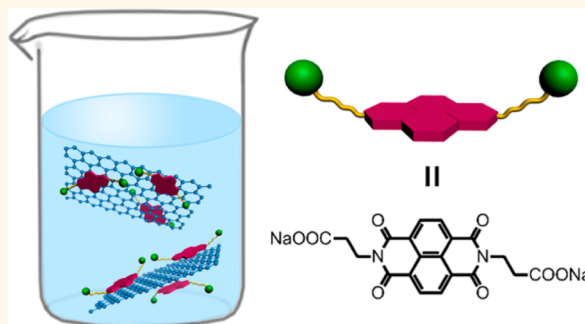


# Rationally Designed Surfactants for Few-Layered Graphene Exfoliation: Ionic Groups Attached to Electron-Deficient $\pi$ -Conjugated Unit through Alkyl Spacers

Lu Zhang,<sup>†</sup> Zijian Zhang,<sup>†,‡</sup> Chaozheng He,<sup>‡</sup> Liming Dai,<sup>§</sup> Jun Liu,<sup>†,\*</sup> and Lixiang Wang<sup>†</sup>

<sup>†</sup>State Key Laboratory of Polymer Physics and Chemistry, Changchun Institute of Applied Chemistry, Chinese Academy of Sciences, Changchun 130022, People's Republic of China, <sup>‡</sup>Physics and Electronic Engineering College, Nanyang Normal University, Nanyang 473061, People's Republic of China, <sup>§</sup>Department of Macromolecular Science and Engineering, Case School of Engineering, Case Western Reserve University, 10900 Euclid Avenue, Cleveland, Ohio 44106, United States, and <sup>†</sup>University of the Chinese Academy of Sciences, Beijing 100049, People's Republic of China

**ABSTRACT** Mass production of graphene with low cost and high throughput is very important for practical applications of graphene materials. The most promising approach to produce graphene with low defect content at a large scale is exfoliation of graphite in an aqueous solution of surfactants. Herein, we report a molecular design strategy to develop surfactants by attaching ionic groups to an electron-deficient  $\pi$ -conjugated unit with flexible alkyl spacers. The molecular design strategy enables the surfactant molecules to interact strongly with both the graphene sheets and the water molecules, greatly improving graphene dispersion in water. As the result, a few-layered graphene concentration as high as 1.2–5.0 mg mL<sup>-1</sup> is demonstrated with the surfactant, which is much higher than those (<0.1 mg mL<sup>-1</sup>) obtained with normal aromatic or nonaromatic surfactants. Moreover, the surfactant can be easily synthesized at large scale. The superior performance and convenient synthesis make the surfactant very promising for mass production of graphene.



**KEYWORDS:** graphene · naphthalene diimide · surfactant · dispersion · ultrasonic exfoliation

Owing to its two-dimensional structure, high surface area, and excellent electrical, thermal, and mechanical properties, graphene has received great attention for various promising applications in energy, composites, biotechnology, and electronics.<sup>1–6</sup> Therefore, low-cost mass production of graphene is essential to meet the demands for the widespread application of graphene materials.<sup>2</sup> Several methods have been devised for graphene preparation, including mechanical cleavage,<sup>1</sup> epitaxial growth,<sup>7</sup> chemical vapor deposition (CVD),<sup>8,9</sup> graphene oxide reduction,<sup>10,11</sup> and liquid-phase graphite exfoliation.<sup>12–25</sup> Because of the low yield and high cost, the mechanical cleavage and the epitaxial growth approaches are unsuitable for a

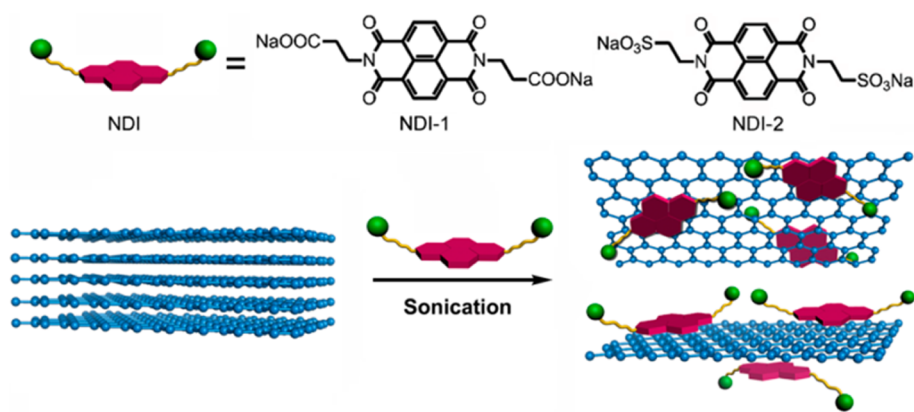
large-scale production of graphene. Similarly, the CVD method has multiple drawbacks, such as low throughput yield and high energy consumption, although it can produce large-area graphene with low defect content. Although the reduction of graphene oxide can give reduced graphene oxide (r-GO) at large scale, the high content of defects in r-GO disrupts the graphene lattice and often leads to graphene of poor quality. Alternatively, the ultrasonication-assisted exfoliation of graphite in solution has been demonstrated to produce high-quality graphene in large quantities.<sup>12–24</sup> The graphite exfoliation can be carried out either in organic solvents with proper surface energies (e.g., *N*-methyl-2-pyrrolidone (NMP) and *N*-dimethylformamide (DMF))<sup>12</sup>

\* Address correspondence to liujun@ciac.jl.cn.

Received for review December 18, 2013 and accepted June 26, 2014.

Published online June 26, 2014  
10.1021/nn502289w

© 2014 American Chemical Society



**Scheme 1.** Schematic illustration for chemical structures of the naphthalene diimide (NDI) surfactants (top) and exfoliation and stabilization of graphene by the surfactants in aqueous solution (bottom).

or in aqueous solution with surfactants.<sup>14</sup> In view of the high cost, high boiling point, and high toxicity characteristic of these organic solvents, we believe that graphite exfoliation in an aqueous solution of surfactants is more suitable for mass production of graphene. However, this approach is still limited by the agglomeration of the exfoliated hydrophobic graphene sheets in aqueous solution, leading to a low concentration of graphene (typically,  $<0.1 \text{ mg mL}^{-1}$ ).<sup>14</sup> Recently, great efforts have been devoted to improve the dispersion stability of the exfoliated graphene in aqueous solution by using effective surfactants. Therefore, the development of novel surfactants for graphene dispersion is of paramount importance for the mass production and practical application of graphene materials.

It is worthy to note that the surfactants reported for graphene dispersion are always borrowed from the field of single-walled carbon nanotube (SWCNT) dispersions.<sup>13–17,26,27</sup> However, the surfactants suitable for the dispersion of one-dimensional SWCNTs with a curved surface may not always be suitable for dispersing two-dimensional graphene with a flat surface. According to Wenseleers *et al.*, for instance, an efficient SWCNT dispersion requires a stable micelle structure of surfactants surrounding nanotubes with a small diameter, but this principle is obviously not applicable to the dispersion of graphene.<sup>28,29</sup> Recently, several large, ionic aromatic molecules have been employed for ultrasonic exfoliation of graphene in aqueous solution.<sup>19–24</sup> Besides their tedious synthesis procedures, these aromatic surfactants show a limited capability for dispersing graphene with a graphene concentration always less than  $0.1 \text{ mg mL}^{-1}$ .

In this Article, we report a novel strategy to design effective surfactants to greatly improve the dispersion ability of graphene in aqueous solution. As shown in Scheme 1, the surfactant molecules are featured with ionic groups covalently attached to a large, electron-deficient aromatic unit with flexible alkyl spacers. The electron-deficient aromatic unit acts as the anchoring unit for absorption of the surfactant molecule onto the

graphene surface *via*  $\pi$ – $\pi$  interaction, hydrophobic force, and Coulomb attraction with the hydrophobic electron-rich graphene surface.<sup>30,31</sup> The ionic groups enable the surfactants and the graphene sheets to be well dispersed in water. The presence of flexible alkyl spacers between the anchoring unit and the ionic groups ensures the two units function well independently. The synergetic effect of these functional units enables strong interactions of the surfactant molecules with both graphene sheets and water molecules and, hence, improves the dispersion of graphene in water. As a result, ultrasonic exfoliation of pristine graphite in an aqueous solution of the surfactants affords a graphene dispersion with the few-layered graphene concentration as high as  $1.2$ – $5.0 \text{ mg mL}^{-1}$ , which is much higher than that ( $<0.1 \text{ mg mL}^{-1}$ ) of pristine graphite exfoliation with other aromatic or nonaromatic surfactants.<sup>17–24</sup> In addition, the novel surfactants can be synthesized in two steps with high yields and can be easily scaled up. The excellent performance and convenient synthesis of the novel surfactants make them very promising for the mass production of graphene.

## RESULTS AND DISCUSSION

As can be seen in Scheme 1, the two rationally designed naphthalene diimide surfactants *N,N'*-bis[2-(ethanoic acid sodium)]-1,4,5,8-naphthalene diimide (NDI-1) and *N,N'*-bis[2-(ethanesulfonic acid sodium)]-1,4,5,8-naphthalene diimide (NDI-2) contain ionic  $-\text{COONa}$  groups or  $-\text{SO}_3\text{Na}$  groups covalently bonded to an NDI unit through ethylene spacers. Naphthalene diimide is selected as the anchoring unit because of its planar structure with a large, electron-deficient  $\pi$ -system. Ethylene is used as the flexible spacer to link the ionic groups with the anchor unit.

To evaluate our molecular design strategy, we calculated the absorption free energies of several surfactants on the graphene surface using periodic density functional theory (DFT) calculations. The surfactants include NDI-2, *N,N'*-bis(ethyl)-3-sulfonic acid sodium-1,4,5,8-naphthalene diimide (NDI-0), 1-pyrenesulfonic

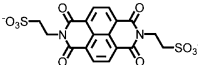
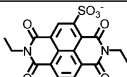
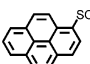
acid sodium salt (PSA), and sodium dodecylbenzenesulfonate (SDBS). Their chemical structures and absorption free energies on the graphene surface are shown in Table 1. SDBS is widely used for SWCNT dispersion, and PSA is a well-known efficient surfactant to disperse graphene. In comparison, NDI-2 and NDI-0 have larger adsorption free energies than those of SDBS and PSA, indicating the strong affinity of the naphthalene diimide unit to the graphene surface. This may be attributed to the large, electron-deficient  $\pi$ -conjugated aromatic system of the naphthalene diimide unit. Furthermore, the larger absorption free energy of NDI-2 compared with NDI-0 suggests the importance of the ethylene spacer, which may diminish the steric effect of bulky  $-\text{SO}_3\text{H}$  groups and favor the adsorption of the naphthalene diimide unit on the graphene surface. The comparison of the absorption free energies of the surfactants supports our molecular design strategy of attaching ionic groups to large, electron-deficient aromatic units with flexible alkyl spacers.

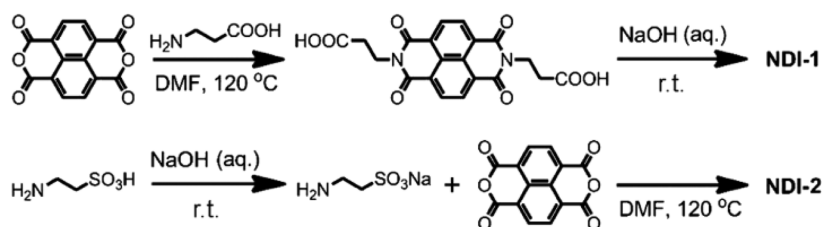
The synthetic routes to NDI-1 and NDI-2 are shown in Scheme 2, and the detailed synthesis procedures can be found in the Materials and Methods. Their chemical structures are verified by  $^1\text{H}$  NMR,  $^{13}\text{C}$  NMR (Figures S1 and S2), and elemental analysis. Both NDI-1 and NDI-2 can be readily synthesized *via* two steps with overall yields higher than 80%. No column chromatography is

required for their purification during synthesis. Thus, the synthesis of NDI-1 and NDI-2 can be easily scaled up, which is highly desirable for low cost and mass production of the surfactants and the exfoliated graphene (Figure S3).

To test the dispersion capability of NDI-1 and NDI-2 surfactants, we carried out ultrasonication exfoliation of pristine graphite in an aqueous solution of the surfactants. Owing to the excess of pristine graphite, centrifugation was performed to remove the unexfoliated graphite and poorly exfoliated graphite. After centrifugation, the exfoliated graphene was kept in the supernatant. The graphene concentration of the supernatant is calculated based on its absorption spectrum (see the Materials and Methods).<sup>12</sup> As shown in Figure 1a, at the optimal NDI-1 concentration of  $4\text{ mg mL}^{-1}$ , a graphene dispersion with a concentration of  $1.2\text{ mg mL}^{-1}$  is obtained after sonication for 1 h and centrifugation at 5000 rpm for 30 min. The graphene concentration depends on the centrifugation speed (Figure 1b). A lower centrifugation speed leads to a higher graphene concentration because larger graphene flakes are retained in the supernatant.<sup>32</sup> Graphene concentrations as high as  $5.0$  and  $2.6\text{ mg mL}^{-1}$  are obtained with centrifugation speeds of 1000 and 3000 rpm, respectively. With the increase of the surfactant concentration, the graphene concentration initially increased and then decreased, giving the optimal surfactant concentration of  $4\text{ mg mL}^{-1}$  (Figure 1a). A similar trend is also observed for the dependence of the zeta potential on the surfactant concentration (Figure 2a), indicating that the graphene sheets in the solution are stabilized by the electrostatic repulsive interactions of the ionic groups of the surfactant molecules. The initial increase of the graphene concentration and zeta potential with increasing surfactant concentration is due to the more available surfactant molecules that can be adsorbed on the graphene surface. Further increasing the surfactant concentration beyond the optimal concentration retarded dissociation of the ionic groups in the surfactant molecules, leading to a decreased graphene concentration and zeta potential.<sup>33</sup> The dispersion of graphene in the aqueous solution of the surfactant is verified by the Tyndall effect shown in Figure S4. The graphene dispersion in the NDI-1 solution is quite stable, as revealed by an only 8% decrease in its absorbance even after storage in ambient conditions for four months (Figure 2b). Compared to NDI-2, NDI-1 exhibits a much better graphene

**TABLE 1. Absorption Free Energies of Four Surfactants on the Graphene Surface Estimated by Periodic DFT Calculations**

Chemical structure	Absorption free energy on graphene surface (eV)
	-1.074
	-0.610
	-0.439
$\text{CH}_3(\text{CH}_2)_{10}\text{CH}_2-\text{C}_6\text{H}_4-\text{SO}_3^-$	-0.273



**Scheme 2. Synthetic routes of NDI-1 and NDI-2 surfactants.**

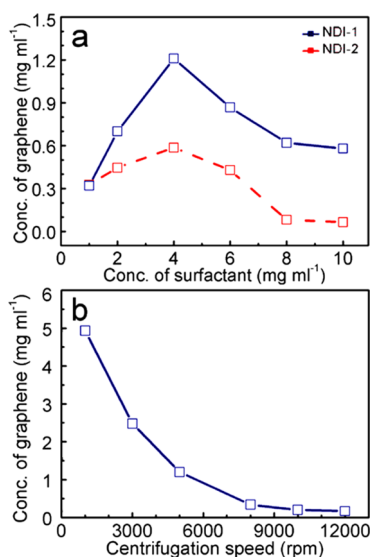


**Figure 1.** (a) Dependence of graphene concentration on the surfactant concentration after centrifuging at 5000 rpm. (b) Dependence of graphene concentration on centrifugation speed for the supernatant after graphite exfoliation in 4 mg mL<sup>-1</sup> NDI-1 aqueous solution.

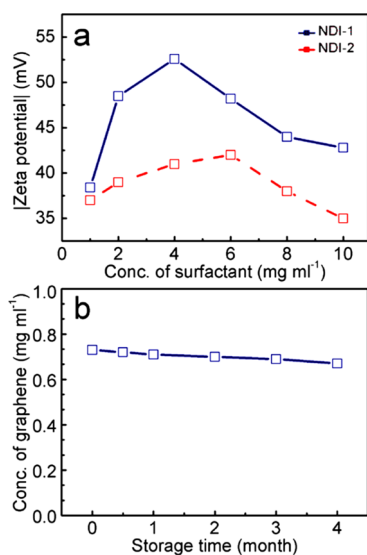


**Figure 2.** (a) Dependence of zeta potential absolute value of graphene sheets on the surfactant concentration after centrifuging at 5000 rpm. (b) Dependence of the NDI-1-stabilized graphene concentration on storage time.

dispersion capability, probably due to the higher solubility of NDI-1 (78.0 mg mL<sup>-1</sup>) than that of NDI-2 (5.2 mg mL<sup>-1</sup>) in water. In addition, owing to the simple synthesis procedures, the surfactants could be prepared in large quantity and the ultrasonic exfoliation of graphite could be performed at large scale (Figure S3).

The observed graphene concentration of 1.2–5.0 mg mL<sup>-1</sup> in NDI-1 aqueous solution is much higher than those (<0.1 mg mL<sup>-1</sup>) obtained by exfoliation of pristine graphite with normal nonaromatic surfactants or ionic aromatic molecules, such as sodium cholate, pyrene derivatives, perylenebisimide-based bolaamphiphile, and coronene tetracarboxylic acid.<sup>20–24</sup>

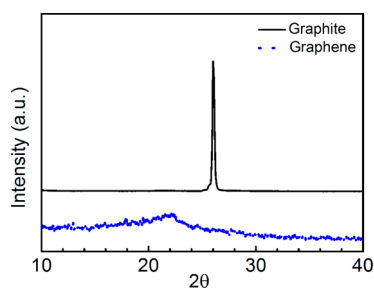


**Figure 3.** XRD patterns for pristine graphite and exfoliated graphene.

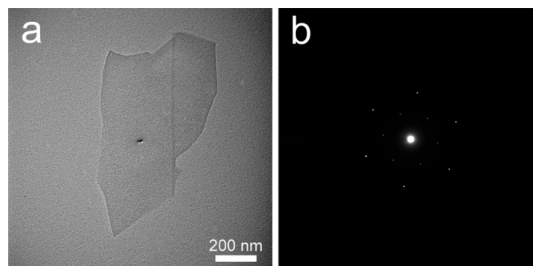


**Figure 4.** TEM image (a) and SAED pattern (b) of an NDI-1-stabilized few-layered graphene flake.

Moreover, the graphene concentration from exfoliation of pristine graphite is even higher than those (0.1–1 mg mL<sup>-1</sup>) from exfoliation of expandable or expanded graphite (H<sub>2</sub>SO<sub>4</sub>/HNO<sub>3</sub> intercalated graphite with graphene sheets oxidized).<sup>18,34,35</sup> The results indicate that NDI-1 is a very effective surfactant to promote the exfoliation of graphite and graphene dispersion in water. The excellent performance of NDI surfactants can be attributed to their unique chemical structures, which enable strong interactions with both graphene sheets and water molecules. The large, electron-deficient  $\pi$ -conjugated NDI unit can strongly adhere to the graphene surface through the  $\pi$ - $\pi$  interaction, hydrophobic force, and the Coulomb attraction with the electron-rich graphene. The ionic -COO<sup>-</sup>/-SO<sub>3</sub><sup>-</sup> groups, generated from dissociation of -COONa/-SO<sub>3</sub>Na units in water, lead to strong solvation with water molecules and prevent the restacking of graphene flakes. The flexible ethylene spacers between the ionic and NDI units enable the two functional units to work independently with a synergistic effect.<sup>36</sup>

The graphene prepared by ultrasonic exfoliation in the NDI-1 aqueous solution was characterized by X-ray diffraction (XRD), transmission electron microscopy (TEM), scanning electron microscopy (SEM), atomic force microscopy (AFM), Raman spectroscopy, etc. As shown in Figure 3, in contrast to the sharp diffraction peak at 26.4° of graphite, the XRD pattern of the exfoliated graphene shows a broad and weak peak at 22.5°, suggesting the efficient exfoliation of graphite.<sup>37</sup> Figure 4a shows the TEM image of an NDI-1-stabilized graphene flake, and the corresponding selected area electron diffraction (SAED) pattern indicates the typical

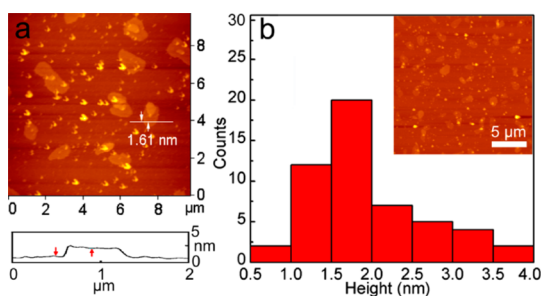


**Figure 5.** (a) AFM image (top) of the few-layered graphene flakes deposited on a mica substrate. Bottom: Height profile corresponding to the line shown in the AFM image. (b) Thickness distribution of 50 graphene flakes in the inset AFM image.

hexagonally arranged lattice of graphene (Figure 4b). The intensity of spots in the second layer is stronger than that in the inner layer, suggesting the presence of the few-layered graphene.<sup>38</sup> Figure 5a shows the AFM image of graphene flakes deposited on a mica substrate, indicating a typical lateral size of around one micron and a thickness of about 1.6 nm. The typical lateral size of graphene flakes in the SEM image (Figure S6a) is in accordance with the results obtained by AFM analysis. According to the thickness distribution of 50 graphene flakes (Figure 5b), the majority of graphene flakes have a thickness of 1.5–2.0 nm, indicating the few-layered graphene flakes (Figure 5b). About 6% of the graphene flakes are single-layered with a thickness of about 1.0 nm.<sup>39</sup> The particles in the AFM images are attributed to the excess surfactants that are not absorbed on the graphene surface. Pure graphene without surfactant is obtained by filtration of the few-layered graphene dispersion and carefully washing the solid with deionized water and ethanol. The absence of the surfactant is verified by the thermal gravimetric analysis (TGA) curve of the few-layered graphene (Figure S7). Figure 6 displays the Raman spectra of graphite and the few-layered graphene with excitation at 514 nm. The G band at about  $1580\text{ cm}^{-1}$  and the D band at about  $1350\text{ cm}^{-1}$  are attributed to the  $\text{sp}^2$ -hybridized carbon bonds in the graphene lattice and the edges/defects in the lattice, respectively. The few-layered graphene flakes show a little stronger D band compared with the pristine graphite, indicating the presence of an edge and/or basal defect induced by ultrasonication exfoliation.<sup>40</sup> The featured 2D band at  $2695\text{ cm}^{-1}$  and the larger intensity ratio of the 2D band to the G band ( $I_{2D}/I_G$ ) suggest the few-layered graphene. Figure 7 displays the XPS spectra of the few-layered graphene flakes, which show a predominate C=C peak at 284.5 eV. The weak signals for the C–C band (285.3 eV), C–O band (286.0 eV), and COOH band (288.9 eV) confirm the low content of defects in the few-layered graphene. We prepared a film of graphene flakes by vacuum filtration to measure the conductivity of the graphene flakes with the

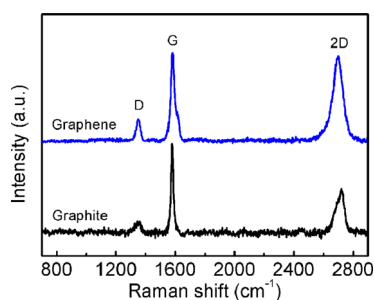


**Figure 6.** Raman spectra of pristine graphite and few-layered graphene.

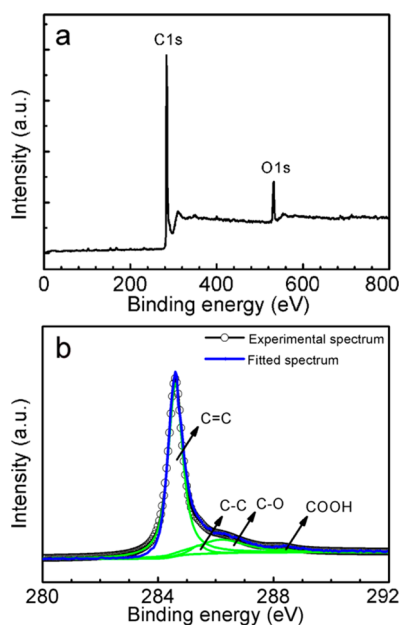


**Figure 7.** XPS full spectrum (a) and C 1s (b) spectrum of few-layered graphene.

four-point probe technique. Figure S6b–d shows the SEM images of the graphene film. The conductivity of the few-layered graphene flakes is measured to be  $4717\text{ S m}^{-1}$ , which is superior to that of graphene prepared by the solution process.<sup>36,41</sup> The high conductivity value may be attributed to the low defect content of the graphene flakes. The specific surface area (SSA) of the few-layered graphene flakes is calculated to be  $53.57\text{ m}^2\text{ g}^{-1}$  based on the  $\text{N}_2$  adsorption–desorption isotherm of graphene flakes as shown in Figure S5. The small SSA value is due to the agglomeration of the few-layered graphene flakes after the removal of surfactants in the solid state.

## CONCLUSION

In conclusion, novel rationally designed NDI surfactants with ionic groups attached to the naphthalene diimide unit through flexible alkyl spacers have been developed for graphene dispersion in an aqueous solution. The NDI surfactants exhibit an excellent capability to exfoliate graphite and disperse graphene in

an aqueous solution, as revealed by the few-layered graphene concentration as high as 5 mg mL<sup>-1</sup> after centrifuging at 1000 rpm or 1.2 mg mL<sup>-1</sup> after centrifuging at 5000 rpm. The superior performance of the surfactants is attributed to their chemical structures, which enable strong interactions with both graphene sheets and water molecules. Therefore, the molecular design strategy, *i.e.*, attaching ionic groups to

the electron-deficient  $\pi$ -conjugated unit *via* flexible spacers, will be generally applicable to develop many surfactants for producing and processing graphene in solution. In addition, the NDI surfactants reported here can be conveniently synthesized and easily scaled up at low cost. Its superior performance and easy synthesis are very desirable for the mass production of graphene with high quality.

## MATERIALS AND METHODS

**Materials.** Natural graphite powder was purchased from Beijing Yuceda Trade Co., Ltd. (325 meshes) and used without further treatment. 1,4,5,8-Naphthalenetetracarboxylic dianhydride (98%) was obtained from Sinopharm Chemical Reagent Co., Ltd.  $\beta$ -Alanine (99%) and taurine (99%) were purchased from Aladdin and used as received.

**Characterizations.** <sup>1</sup>H NMR and <sup>13</sup>C NMR spectra were recorded with a Bruker Avance 300 NMR spectrometer. TEM images were obtained with a JEM-1011 (JEOL Co., Japan) operated at an accelerating voltage of 100 kV. The samples for TEM measurements were made by depositing a graphene dispersion on carbon-coated copper grids (300 meshes), followed by drying in air for 1 min. AFM in tapping model was performed with an SPI 3800N Probe Station (Seiko Instruments Inc., Japan). The sample for AFM measurement was prepared by spin-coating the graphene dispersion (0.1 mg mL<sup>-1</sup>) onto a silica substrate at 2000 rpm for 1 min. SEM imaging was performed on a Philips-FEI XL30 microscope at an accelerating voltage of 20 kV. The sample of graphene flakes was prepared by spin-coating the graphene dispersion (0.1 mg mL<sup>-1</sup>) onto a silica substrate at 2000 rpm for 1 min. Graphene film was prepared by vacuum filtration of a few-layered graphene dispersion with a polyvinylidene fluoride membrane (pore size: 0.45  $\mu$ m), followed by careful washing with deionized water and ethanol to remove the surfactant and drying under vacuum at 120 °C for 3 h. The obtained graphene film and the used graphene flakes are shown in the SEM images of Figure S6. The XRD patterns of the pristine graphite and the graphene film were collected on a Rigaku-D/max 2500 V X-ray diffractometer with Cu K $\alpha$  radiation. XPS measurement was carried out with the graphene film using a VG EscalabmkII spectrometer (UK) with an Al K $\alpha$  irradiation source (1486.7 eV) operated at 15 kV and 10 mA. Raman spectrum was recorded with the graphene film using a Renishaw Raman microscope equipped with a 514 nm Ar ion laser. With the sheet resistance ( $R_s$ ) of the graphene film measured by a Keithley 2000 multimeter and the thickness ( $t$ ) estimated by an optical microscope (Leica DMLP, Leica Microsystems Ltd., Germany), the conductivity ( $\rho$ ) of the graphene sample was calculated with the equation  $\rho = R_s \times t$ . UV-vis absorption was recorded using a PerkinElmer Lambda 35 UV-vis spectrometer. The thermal stability of graphene was analyzed with a PerkinElmer-TGA 7 instrument under nitrogen flow at a heating rate of 10 °C min<sup>-1</sup>. Zeta potential values were obtained using a Zetasizer analyzer (Nano-ZS90, Malvern, France). During the measurement of the zeta potential, graphene dispersions with different concentrations were diluted to nearly the same concentration. The N<sub>2</sub> adsorption-desorption isotherm was acquired at 77 K with a Micromeritics ASAP 2010 M instrument, and the specific surface area was calculated by the Brunauer-Emmett-Teller method.

**Simulation Method.** In the present work, periodic DFT calculations were carried out with the Vienna *ab initio* simulation package (VASP). The exchange-correlation energies were dealt with by the generalized gradient approximation (GGA) with the function of Perdew and Wang (PW91), and electron-ion interactions were described by the projected augmented wave (PAW) method. We used a plane wave basis set with an energy cutoff of 400 eV. Spin-polarized calculations were carried out.

The  $\Gamma$ -point was chosen in the Brillouin zone integration for a larger 10  $\times$  10 supercell of graphene, which contains 200 carbon atoms. The slab supercell considered has been carefully tested, and a 30 Å vacuum along the *c* axis has been adopted to ensure no reciprocal interaction between periodic images. All the atoms of graphene were allowed to relax along with the adsorbates, and the optimization was stopped when the root-mean-square force on the atomic nuclei was less than 0.05 eV Å<sup>-1</sup>. The adsorption energies ( $E_{ad}$ ) for all possible adsorbates were calculated according to

$$E_{ad} = E_{gas-graphene} - (E_{gas} + E_{graphene})$$

where  $E_{gas-graphene}$ ,  $E_{gas}$ , and  $E_{graphene}$  are total energies of the adsorbed species on graphene, the clean graphene surface, and the corresponding gas-phase species, respectively.

**Synthesis of NDI-1.** A mixture of 1,4,5,8-naphthalenetetracarboxylic dianhydride (5.39 g, 20 mmol),  $\beta$ -alanine (5.29 g, 60 mmol), and DMF (60 mL) was stirred at 120 °C for 10 h. After cooling to room temperature, the precipitate was filtered off, washed sequentially with water and methanol, and dried in a vacuum to afford *N,N'*-bis[2-(ethanoic acid)]-1,4,5,8-naphthalene diimide (**1**). Then an aqueous solution (80 mL) of **1** (3.50 g, 8.54 mmol) was added dropwise into an aqueous NaOH solution (0.1 M, 170 mL, 0.17 mmol). After removing the solvent, the residue was recrystallized in water/ethanol to afford the title compound. Overall yield: 7.48 g (81.9%). <sup>1</sup>H NMR (300 MHz, D<sub>2</sub>O,  $\delta$ , ppm): 8.43 (s, 4H), 4.28 (t, 4H), 2.54 (t, 4H). <sup>13</sup>C NMR (75 MHz, D<sub>2</sub>O,  $\delta$ , ppm): 179.65, 163.13, 130.83, 125.51, 125.17, 38.07, 35.23. Anal. Calcd for C<sub>20</sub>H<sub>12</sub>N<sub>2</sub>O<sub>8</sub>Na<sub>2</sub>: C, 52.88; H, 2.66; N, 6.17. Found: C, 52.90; H, 2.87; N, 6.04.

**Synthesis of NDI-2.** Aminoethanesulfonic acid (7.51 g, 60 mmol) was neutralized with NaOH (2.40 g, 60 mmol) in aqueous solution (200 mL) to afford aminoethanesulfonic sodium. Then a mixture of aminoethanesulfonic sodium (8.82 g, 59.9 mmol) and 1,4,5,8-naphthalenetetracarboxylic acid dianhydride (7.94 g, 29.6 mmol) in DMF (250 mL) was stirred at 120 °C for 20 h. After cooling to room temperature, the precipitate was filtered off and washed sequentially with DMF and ethanol. Recrystallization in water/ethanol afforded the title compound as a light yellow solid. Yield: 13.98 g (89.7%). <sup>1</sup>H NMR (300 MHz, D<sub>2</sub>O,  $\delta$ , ppm): 8.50 (s, 4H), 4.47 (t, 4H), 3.27 (t, 4H). <sup>13</sup>C NMR (75 MHz, D<sub>2</sub>O,  $\delta$ , ppm): 164.09, 131.75, 126.52, 126.45, 48.71, 37.05. Anal. Calcd for C<sub>18</sub>H<sub>12</sub>N<sub>2</sub>O<sub>10</sub>S<sub>2</sub>Na<sub>2</sub>: C, 41.17; H, 2.30; N, 5.32. Found: C, 41.06; H, 2.26; N, 5.19.

**Ultrasonic Exfoliation of Graphite in the Surfactant Aqueous Solution.** Ultrasonic exfoliation of graphite was carried out using a 20 kHz, horn-type ultrasonic homogenizer (Scientz-IIID, Ningbo Xingzhi Biotechnology Co., Ltd.) with a 0.07 cm<sup>2</sup> titanium alloy sonotrode tip. A mixture of the pristine graphite powder (0.5 g), NDI surfactant of specific weight, and deionized water (5.0 mL) was sonicated for 1 h in an ice-water bath. The mixture was then centrifuged at 5000 rpm for 30 min. The graphene dispersion obtained with the optimal NDI-1 surfactant concentration of 4 mg mL<sup>-1</sup> and the centrifugation at 5000 rpm for 30 min was used for all the characterizations.

**Determination of Graphene Concentration Using Absorbance.** The absorption coefficient ( $R$ ) of graphene at 660 nm was determined based on the exact concentration of a graphene dispersion and the absorbance at 660 nm. A graphene dispersion (20 mL) was vacuum filtered with a preweighed membrane with

a pore size of 0.45  $\mu\text{m}$ . The solid was thoroughly washed with deionized water and ethanol to completely remove the surfactant (the complete removal of the surfactant was confirmed by TGA, shown in Figure S7). After drying, the membrane was reweighed to give the deposited mass; thus the exact graphene concentration (C) in the dispersion was obtained. For the absorbance measurement, the same graphene dispersion was first diluted by 20 times with deionized water. With the absorbance ( $A_1$ ) at 660 nm of the diluted dispersion measured with UV-vis absorption spectroscopy, the absorbance of the original graphene dispersion (A) was calculated with  $A = 20 \times A_1$ . Therefore, according to the Lambert-Beer law  $A = RCL$ , where L is the light path length, we calculated the R of graphene at 660 nm to be 1506 mL  $\text{mg}^{-1} \text{m}^{-1}$ . Then, the concentration of graphene in each dispersion was determined by measuring its absorbance at 660 nm and calculating with the Lambert-Beer law.

**Conflict of Interest:** The authors declare no competing financial interest.

**Supporting Information Available:** Additional information including  $^1\text{H}$  NMR and  $^{13}\text{C}$  NMR spectra of NDI surfactants, photographs of an NDI-stabilized graphene dispersion at large quantity and Tyndall effect,  $\text{N}_2$  isotherm adsorption-desorption curves, SEM images, and TGA data. This material is available free of charge via the Internet at <http://pubs.acs.org>.

**Acknowledgment.** The authors are grateful for the financial support by the 973 Project (No. 2014CB643504), the Nature Science Foundation of China (No. 51373165), and the "Thousand Talents Program" of China.

## REFERENCES AND NOTES

- Novoselov, K. S.; Geim, A. K.; Morozov, S. V.; Jiang, D.; Zhang, Y.; Dubonos, S. V.; Grigorieva, I. V.; Firsov, A. A. Electric Field Effect in Atomically Thin Carbon Films. *Science* **2004**, *306*, 666–669.
- Geim, A. K.; Novoselov, K. S. The Rise of Graphene. *Nat. Mater.* **2007**, *6*, 183–191.
- Jeon, I.-Y.; Shin, Y.-R.; Sohn, G.-J.; Choi, H.-J.; Bae, S.-Y.; Mahmood, J.; Jung, S.-M.; Seo, J.-M.; Kim, M.-J.; Chang, D. W.; *et al.* Edge-Carboxylated Graphene Nanosheets via Ball Milling. *Proc. Natl. Acad. Sci. U.S.A.* **2012**, *109*, 5588–5593.
- Guo, C. X.; Yang, H. B.; Sheng, Z. M.; Lu, Z. S.; Song, Q. L.; Li, C. M. Layered Graphene/Quantum Dots for Photovoltaic Devices. *Angew. Chem., Int. Ed.* **2010**, *49*, 3014–3017.
- Allen, M. J.; Tung, V. C.; Kaner, R. B. Honeycomb Carbon: A Review of Graphene. *Chem. Rev.* **2010**, *110*, 132–145.
- Dai, L. M. Functionalization of Graphene for Efficient Energy Conversion and Storage. *Acc. Chem. Res.* **2013**, *46*, 31–42.
- Yang, W.; Chen, G.; Shi, Z.; Liu, C. C.; Zhang, L.; Xie, G.; Cheng, M.; Wang, D.; Yang, R.; Shi, D.; *et al.* Epitaxial Growth of Single-Domain Graphene on Hexagonal Boron Nitride. *Nat. Mater.* **2013**, *12*, 792–799.
- Reina, A.; Jia, X. T.; Ho, J.; Nezich, D.; Son, H.; Bulovic, V.; Dresselhaus, M. S.; Kong, J. Large Area, Few-Layer Graphene Films on Arbitrary Substrates by Chemical Vapor Deposition. *Nano Lett.* **2009**, *9*, 30–35.
- Park, S.; Ruoff, R. S. Chemical Methods for the Production of Graphenes. *Nat. Nanotechnol.* **2009**, *4*, 217–224.
- Eda, G.; Fanchini, G.; Chhowalla, M. Large-Area Ultrathin Films of Reduced Graphene Oxide as a Transparent and Flexible Electronic Material. *Nat. Nanotechnol.* **2008**, *3*, 270–274.
- Dreyer, D. R.; Ruoff, R. S.; Bielawski, C. W. From Conception to Realization: An Historical Account of Graphene and Some Perspectives for its Future. *Angew. Chem., Int. Ed.* **2010**, *49*, 9336–9344.
- Hernandez, Y.; Nicolosi, V.; Lotya, M.; Blighe, F. M.; Sun, Z. Y.; DE, S.; McGovern, I. T.; Holland, R.; Byrne, M.; Gun'ko, Y. K. *et al.* High-Yield Production of Graphene by Liquid-Phase Exfoliation of Graphite. *Nat. Nanotechnol.* **2008**, *3*, 563–568.
- Lotya, M.; Hernandez, Y.; King, P. J.; Smith, R. J.; Nicolosi, V.; Karlsson, L. S.; Blighe, F. M.; De, S.; Wang, Z. M.; McGovern, I. T.; *et al.* Liquid Phase Production of Graphene by Exfoliation of Graphite in Surfactant/Water Solutions. *J. Am. Chem. Soc.* **2009**, *131*, 3611–3620.
- Ciesielski, A.; Samori, P. Graphene via Sonication Assisted Liquid-Phase Exfoliation. *Chem. Soc. Rev.* **2014**, *43*, 381–398.
- Liang, Y. T.; Hersam, M. C. Highly Concentrated Graphene Solutions via Polymer Enhanced Solvent Exfoliation and Iterative Solvent Exchange. *J. Am. Chem. Soc.* **2010**, *132*, 17661–17663.
- Wang, X. Q.; Fulvio, P. F.; Baker, G. A.; Veith, G. M.; Unocic, R. R.; Mahurin, S. M.; Chi, M. F.; Dai, S. Direct Exfoliation of Natural Graphite into Micrometre Size Few Layers Graphene Sheets Using Ionic Liquids. *Chem. Commun.* **2010**, *46*, 4487–4489.
- Bourlinos, A. B.; Georgakilas, V.; Zboril, R.; Steriotis, T. A.; Stubos, A. K.; Trapalis, C. Aqueous-Phase Exfoliation of Graphite in the Presence of Polyvinylpyrrolidone for the Production of Water-Soluble Graphenes. *Solid State Commun.* **2009**, *149*, 2172–2176.
- Guardia, L.; Fernández-Merino, M. J.; Paredes, J. I.; Solís-Fernández, P.; Villar-Rodil, S.; Martínez-Alonso, A.; Tascón, J. M. D. High-Throughput Production of Pristine Graphene in an Aqueous Dispersion Assisted by Non-Ionic Surfactants. *Carbon* **2011**, *49*, 1653–1662.
- Parviz, D.; Das, S.; Ahmed, H. S. T.; Irin, F.; Bhattacharia, S.; Green, M. J. Dispersions of Non-Covalently Functionalized Graphene with Minimal Stabilizer. *ACS Nano* **2012**, *6*, 8857–8867.
- Nayak, S. K.; Talapatra, S.; Kar, S. Stable Aqueous Dispersions of Noncovalently Functionalized Graphene from Graphite and their Multifunctional High-Performance Applications. *Nano Lett.* **2010**, *10*, 4295–4301.
- Ghosh, A.; Rao, K. V.; George, S. J.; Rao, C. N. R. Noncovalent Functionalization, Exfoliation, and Solubilization of Graphene in Water by Employing a Fluorescent Coronene Carboxylate. *Chem.—Eur. J.* **2010**, *16*, 2700–2704.
- Englert, J. M.; Rohrl, J.; Schmidt, C. D.; Graupner, R.; Hundhausen, M.; Hauke, F.; Hirsch, A. Soluble Graphene: Generation of Aqueous Graphene Solutions. *Adv. Mater.* **2009**, *21*, 4265–4269.
- Lee, D. W.; Kim, T.; Lee, M. An Amphiphilic Pyrene Sheet for Selective Functionalization of Graphene. *Chem. Commun.* **2011**, *47*, 8259–8261.
- Sampath, S.; Basuray, A. N.; Hartlieb, K. J.; Aytun, T.; Stupp, S. I.; Stoddart, J. F. Direct Exfoliation of Graphite to Graphene in Aqueous Media with Diazaperopyrenium Dications. *Adv. Mater.* **2013**, *25*, 2740–2745.
- Edwards, R. S.; Coleman, K. S. Graphene Synthesis: Relationship to Applications. *Nanoscale* **2013**, *5*, 38–51.
- Ehli, C.; Rahman, G. M. A.; Jux, N.; Balbinot, D.; Guldi, D. M.; Paolucci, F.; Marcaccio, M.; Paolucci, D.; Melle-Franco, M.; Zerbetto, F.; *et al.* Interactions in Single Wall Carbon Nanotubes/Pyrene/Porphyrin Nanohybrids. *J. Am. Chem. Soc.* **2006**, *128*, 11222–11231.
- Lu, J.; Yang, J. X.; Wang, J. Z.; Lim, A.; Wang, S.; Loh, K. P. One-Pot Synthesis of Fluorescent Carbon Nanoribbons, Nanoparticles, and Graphene by the Exfoliation of Graphite in Ionic Liquids. *ACS Nano* **2009**, *3*, 2367–2375.
- Wenseleers, W.; Vlasov, J.; Goovaerts, E.; Obraztsova, E. D.; Lobach, A. S.; Bouwen, A. Efficient Isolation and Solubilization of Pristine Single-Walled Nanotubes in Bile Salt Micelles. *Adv. Funct. Mater.* **2004**, *14*, 1105–1112.
- Cardenas, J. F.; Gromoc, A. The Effect of Bundling on the G' Raman Band of Single-Walled Carbon Nanotubes. *Nanotechnology* **2009**, *20*, 465703.
- Zhan, X.; Facchetti, A.; Barlow, S.; Marks, T. J.; Ratner, M. A.; Wasielewski, M. R.; Marder, S. R. Rylene and Related Diimides for Organic Electronics. *Adv. Mater.* **2011**, *23*, 268–284.
- Chen, Z.; Lohr, A.; Saha-Möller, C. R.; Würthner, F. Self-Assembled pi-Stacks of Functional Dyes in Solution: Structural and Thermodynamic Features. *Chem. Soc. Rev.* **2009**, *38*, 564–584.

32. Khan, U.; O'Neill, A.; Porwal, H.; May, P.; Nawaz, K.; Coleman, J. N. Size Selection of Dispersed, Exfoliated Graphene Flakes by Controlled Centrifugation. *Carbon* **2012**, *50*, 470–475.
33. Kim, T.; Lee, H.; Kim, J.; Suh, K. S. Synthesis of Phase Transferable Graphene Sheets Using Ionic Liquid Polymers. *ACS Nano* **2010**, *4*, 1612–1620.
34. Li, X. L.; Zhang, G. Y.; Bai, X. D.; Sun, X. M.; Wang, X. R.; Dai, H. J. Highly Conducting Graphene Sheets and Langmuir-Blodgett Films. *Nat. Nanotechnol.* **2008**, *3*, 538–542.
35. Hamilton, C. E.; Lomeda, J. R.; Sun, Z. Z.; Tour, J. M.; Barron, A. R. High-Yield Organic Dispersions of Unfunctionalized Graphene. *Nano Lett.* **2009**, *9*, 3460–3462.
36. Everett, D. H. *Basic Principles of Colloid Science*; Royal Society of Chemistry: London, 1988; pp 2–244.
37. Chen, W. F.; Yan, L. F. *In Situ* Self-Assembly of Mild Chemical Reduction Graphene for Three-Dimensional Architectures. *Nanoscale* **2011**, *3*, 3132–3137.
38. Meyer, J. C.; Geim, A. K.; Katsnelson, M. I.; Novoselov, K. S.; Booth, T. J.; Roth, S. The Structure of Suspended Graphene Sheets. *Nature* **2007**, *446*, 60–63.
39. Zheng, J.; Di, C. A.; Liu, Y. Q.; Liu, H. T.; Guo, Y. L.; Du, C. Y.; Wu, T.; Yu, G.; Zhu, D. B. High Quality Graphene with Large Flakes Exfoliated by Oleyl Amine. *Chem. Commun.* **2010**, *46*, 5728–5730.
40. Skaltsas, T.; Ke, X. X.; Bittencourt, C.; Tagmatarchis, N. Ultrasonication Induces Oxygenated Species and Defects onto Exfoliated Graphene. *J. Phys. Chem. C* **2013**, *117*, 23272–23278.
41. Xu, Y. X.; Bai, H.; Lu, G. W.; Li, C.; Shi, G. Q. Flexible Graphene Films via the Filtration of Water-Soluble Noncovalent Functionalized Graphene Sheets. *J. Am. Chem. Soc.* **2008**, *130*, 5856–5862.